

# Chemical reactions in liquids: Molecular dynamics simulation for sulfur

Frank H. Stillinger, Thomas A. Weber, and Randall A. LaViolette  
*AT&T Bell Laboratories, Murray Hill, New Jersey 07974*

(Received 4 August 1986; accepted 25 August 1986)

A combination of two-atom and three-atom interactions has been selected to represent the structural chemistry of sulfur. This model potential exhibits divalency (bond saturation) and leads to the known preference for  $S_n$  molecules to form puckered ring structures. Using this representation of the interactions, molecular dynamics calculations have been performed for 1000 sulfur atoms at the experimental liquid density. Short-range order has been calculated for the low-temperature liquid consisting of  $S_8$  cyclic molecules, and agrees qualitatively with the (imprecise) available measurements. At elevated temperatures the cyclic  $S_8$  molecules in the simulation begin to break open, and their subsequent chemical reactions yield primarily linear polymeric species. A metastable reaction intermediate in the polymerization process has been identified, a "tadpole" consisting of a diradical chain attached weakly to an  $S_8$  ring.

## I. INTRODUCTION

The theory of gas-phase chemical reaction rates has become a mature field. For the most part it is conceptually straightforward, comprehensive, and extremely useful for interpreting kinetic measurements.<sup>1,2</sup> By contrast, theory for chemical reaction rates in condensed phases (both liquid and solid) is poorly developed, and its interpretive ability is often weak. This discrepancy arises from ignorance about solvation interactions in condensed phases, about the local structures that those interactions produce, and about the collective motions of coupled reactant and solvent along reaction pathways.

Computer simulation has exerted a powerful and positive influence on the development of fundamental liquid state theory. Simple atomic liquids are now well understood as a result.<sup>3</sup> Furthermore, computer simulation has contributed major insights into the static and dynamic behavior of some important types of polyatomic liquids.<sup>4-6</sup> But excepting a few isolated special cases,<sup>7-9</sup> computer simulation has yet to be applied to study of chemical kinetics in condensed media.

The present paper reports our initial progress in attempting to model liquid sulfur. This elemental substance offers an attractive challenge because of the diversity of stable molecules  $S_n$  ( $n > 5$ ) that it can form,<sup>10</sup> and because of the rich allotropy displayed by the corresponding crystalline states.<sup>11</sup> Furthermore chemical conversions of the molecular species occur at convenient rates under reasonable temperature conditions, and have been widely studied in the laboratory.<sup>12</sup> Finally, liquid sulfur exhibits a fascinating transition at 159 °C in its liquid phase, at which various physical properties show dramatic singularities.<sup>13</sup>

We have been obliged to undertake, in sequence, a pair of tasks. The first is to identify a generic potential energy function for an arbitrary collection of sulfur atoms which approximately reproduces the structural chemistry of that element. Most importantly this means achieving divalency for sulfur chemical bonding, with vertex and dihedral angle preferences such that  $S_n$  rings and helical polymers can readily form. The second task requires using the selected

potential function in a molecular dynamics simulation of the liquid phase. It is necessary to demonstrate that a liquid composed of cyclic  $S_8$  molecules at low temperature has (on the molecular dynamics time scale) long-time chemical stability, but that at elevated temperature chemical reactions spontaneously occur to alter the populations of molecular species.

The results reported below yield a provocative connection between chemical reactivity, and the so-called "inherent structure" general formalism for the liquid state.<sup>14-17</sup> The latter resolves observed short-range order into a packing component that is associated with potential energy minima for the substance of interest, and a component due to vibrational distortions away from those minima. We now see, for sulfur at least, that all potential energy minima (packings) as well as their associated basins of vibrational distortion can be uniquely and unambiguously classified according to which molecular species are present.

Section II presents the specific choice of two-body and three-body potential functions which we have used to represent sulfur atom interactions. Cluster structures and energies implied by this choice are presented as well.

On account of interest in reactivity, Sec. III is devoted to locating and examining transition states for ring opening. Constrained optimizations have been carried out for bond stretch and breakage in (initially) cyclic  $S_6$  and  $S_8$ .

The molecular dynamics protocols have been summarized in Sec. IV. The results of our simulations then appear in Sec. V. These have involved distinct initial conditions and a wide range of temperatures to establish qualitatively that the model behaves properly. Section VI discusses properties of quenched structures prepared from the molecular dynamics states.

Section VII summarizes our progress and comments on its implications for the future.

## II. MODEL INTERACTION

Previous work devoted to the modeling of silicon<sup>18</sup> demonstrates that valence saturation with directed chemical bonds can be mathematically represented with a combina-

tion of two-atom ( $v_2$ ) and three-atom ( $v_3$ ) interactions. While recognizing that divalent sulfur requires a different balance of such interactions than does tetravalent silicon, we have elected to use the same functional format. Consequently, the potential energy  $\Phi$  for an arbitrary configuration of  $N$  sulfur atoms will be written as follows:

$$\Phi = \sum_{i < j = 1}^N v_2(r_{ij}) + \sum_{i < j < k = 1}^N v_3(r_i, r_j, r_k). \quad (2.1)$$

Both experimental data and computational prudence have been invoked in selection of  $v_2$  and  $v_3$ . The former includes (a) dissociation energy (100.797 kcal/mol) for diatomic sulfur  $S_2^{19}$ ; (b) mean bond length (2.06 Å), mean bond vertex angle (108°), and mean dihedral angle (85°) observed in crystals of  $S_8$ .<sup>11</sup> The latter suggests using simple combinations of elementary functions, with a strict but smooth cutoff at modest range.

After considerable experimentation with alternative forms, we discovered that the following  $v_2$  and  $v_3$  perform adequately in representing the structural chemistry of sulfur. Using reduced units (energy unit  $\epsilon = 100.797$  kcal/mol, length unit  $\sigma = 1.6836$  Å),

$$\begin{aligned} v_2(r) &= 15.339\,214(r^{-2} - 0.16) \\ &\quad \times (r^{-2} - 0.25)(r^{-2} - 1.077) \\ &\quad \times \exp[(r - 3.6)^{-1}] \quad (r < 3.6) \\ &= 0 \quad (r \geq 3.6), \end{aligned} \quad (2.2)$$

$$\begin{aligned} v_3(r_1, r_2, r_3) &= h(r_{12}, r_{13}, \theta_{213}) + h(r_{21}, r_{23}, \theta_{123}) \\ &\quad + h(r_{31}, r_{32}, \theta_{132}), \end{aligned} \quad (2.3)$$

$$\begin{aligned} h(r, s, \theta) &= [75(\cos \theta - \cos 95^\circ)^2 + 25] \\ &\quad \times \exp[3(r - 2.5)^{-1} + 3(s - 2.5)^{-1}] \\ &\quad (r, s < 2.5) \\ &= 0 \quad (\text{otherwise}). \end{aligned} \quad (2.4)$$

Here we have let  $\theta_{jik}$  stand for the angle at atom  $i$  subtended by atoms  $j$  and  $k$ . Notice that both  $v_2$  and  $v_3$  have finite cutoffs at which all derivatives vanish, but that  $v_2$  is substantially longer ranged than  $v_3$ .

Figure 1 provides a plot of the pair function  $v_2$ . This function alone accounts for the chemical bonding in the sulfur dimer. Its minimum (constructed to be  $-1$ ) occurs at reduced distance:

$$r_e(S_2) = 1.122\,36. \quad (2.5)$$

This is equivalent to 1.8896 Å, which may be compared with the measured value 1.8892 Å.<sup>19</sup> Anticipating molecular dynamics results, we point out that this dimeric species at best plays a very minor role in most condensed-phase properties.

Figure 1 shows that  $v_2$  possesses a low maximum and subsequent shallow minimum beyond  $r_e$ . These features are important in controlling the preferred dihedral angles in cyclic  $S_n$  species (see below).

The three-body interaction  $v_3$  is nowhere negative. Its role is to create bond saturation at valence two, utilizing the fact that the number of trimers including a given atom increases more rapidly than linearly with that atom's coordi-

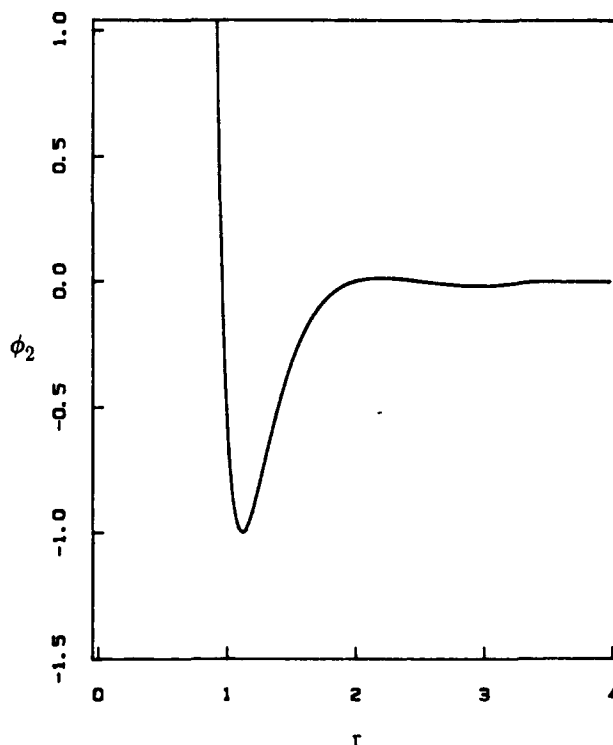


FIG. 1. Atom pair potential (in reduced units) vs distance.

nation number. The angle variation of the component function  $h$  is illustrated in Fig. 2.

Mechanically stable cluster geometries have been extensively examined to verify that  $\Phi$ , Eq. (2.1), captures the main aspects of sulfur structural chemistry. Starting from

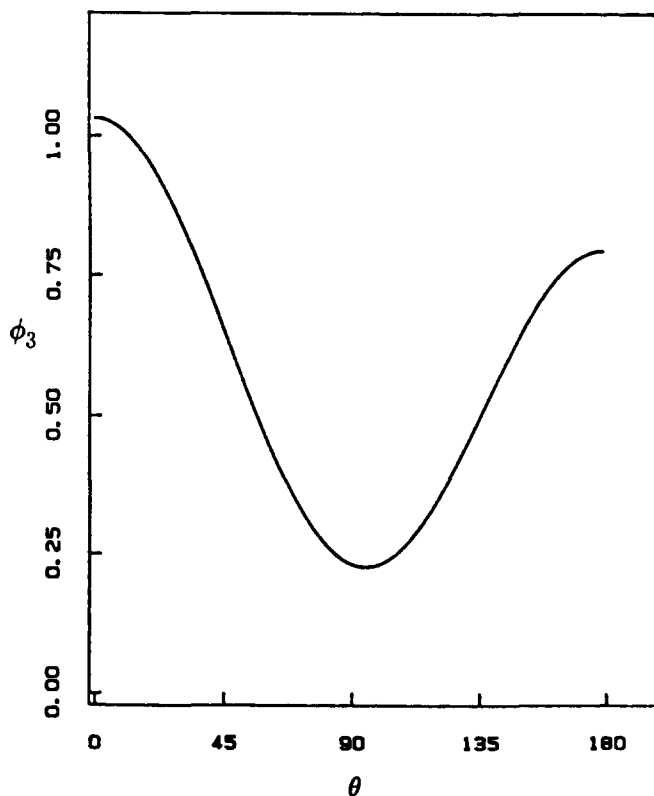


FIG. 2. Angle variation of the trimer-interaction component function  $h(r, s, \theta)$ , with  $r = s = 1.2236$ .

several initial configurations of each of  $n = 3$  to 10, and 12, sulfur atoms, local minima on the corresponding  $\Phi$  hypersurface have been identified by computer using both steepest-descent and quasi-Newton<sup>20</sup> procedures. For  $n \leq 8$  we believe that the search has been sufficiently exhaustive to have uncovered the lowest-energy structures; for larger  $n$  we are less confident that this is so.

The lowest-energy minimum for  $S_3$  has potential energy equal to  $-1.5146$ . The molecular structure at this minimum is an isosceles triangle with bond lengths equal to 1.1659 (i.e., 1.9629 Å) and vertex angle between these bonds equal to  $110.4^\circ$ . The sulfur trimer is also predicted to have a higher-lying  $\Phi$  minimum at  $-1.2471$ , with equilateral geometry and bond lengths 1.2017 (2.0232 Å).

The most stable configuration for  $S_4$  is a nonplanar chain of three covalent bonds, whose lengths in reduced units are 1.1561, 1.2570, and 1.1561. The bond angles in this structure are  $110.9^\circ$ , the dihedral angle is  $112.1^\circ$ , and the end-to-end distance accordingly is 2.7406. This chiral unit has  $\Phi$  equal to  $-2.0822$ . The square planar arrangement for  $S_4$  corresponds to a higher-lying relative minimum in  $\Phi$ , at  $-1.7418$ .

When at least five sulfur atoms are present, ring closure is possible without seriously violating the preferred vertex angle (about  $110^\circ$  for the present model). Consequently the minimum- $\Phi$  structure of  $S_5$  is a planar regular pentagon with bonds of length 1.2297 (2.0703 Å).

The global  $\Phi$  minimum for  $S_6$  is achieved in a chair-form puckered hexagon, with bond lengths equal to 1.2199 (2.0538 Å) and vertex angles equal to  $110.3^\circ$ . The corresponding values that have been experimentally observed for puckered  $S_6$  rings in their rhombohedral crystal are  $2.057 \pm 0.018$  Å, and  $102.2 \pm 1.6^\circ$ .<sup>11</sup>

Among the higher-lying  $\Phi$  minima for  $S_6$ , we have also found a boat-form hexagon. The energy separation between these conformers is found to be

$$\begin{aligned} \Phi(\text{boat}) - \Phi(\text{chair}) &= 0.01765 \\ &= 1.780 \text{ kcal/mol.} \end{aligned} \quad (2.6)$$

Although this alternative  $S_6$  structure has not been identified in an allotrope of sulfur, speculations regarding its existence and properties have been published.<sup>21</sup>

The most stable form obtained for  $S_7$  in the present model is a nonplanar ring with a single plane of symmetry. This appears to be consistent with crystallographic information for the heptamer.<sup>22</sup>

Orthorhombic sulfur, a crystal consisting of puckered  $S_8$  rings, is the stable low-temperature form of the element. Our lowest-energy octamer also has this puckered ring form, with equivalent bonds of length 1.2236 (2.0601 Å), and vertex angles of  $110.9^\circ$ . The experimental crystal structure is such that molecular symmetry is weakly broken by crystal forces, but average bond length and angle are observed respectively to be  $2.060 \pm 0.003$  Å and  $108.0 \pm 0.7^\circ$ .<sup>11</sup>

Another  $S_8$  ring conformer, lying 0.07148 energy units (7.205 kcal/mol) higher in energy was also achieved. This bears essentially the same relation to the most stable  $S_8$  as does boat-form  $S_6$  to chair-form  $S_6$ : interconversion is

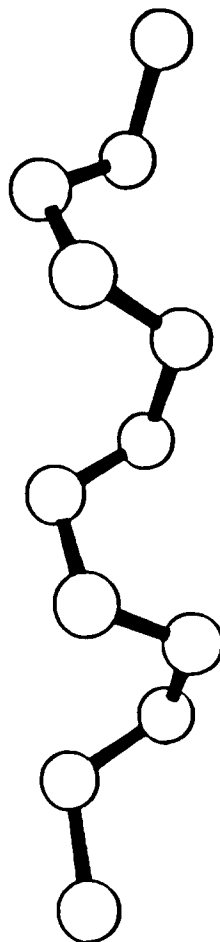


FIG. 3. Helical diradical form for  $S_{12}$ .

achieved by flipping up (or down) one sulfur vertex and its associated bond pair.

Rings of covalently bonded (divalent) sulfur appear to supply the minimum-energy structures for the remaining cases examined, namely  $S_9$ ,  $S_{10}$ , and  $S_{12}$ . This also agrees with crystallographic evidence.<sup>10-12</sup>

An open-chain diradical structure for  $S_{12}$  has also been found to be a mechanically stable form (a local  $\Phi$  minimum). It is shown in Fig. 3. The energy required to break open our (apparently optimal)  $S_{12}$  ring and to stretch it out in this diradical form is 0.20961 energy units (21.128 kcal/mol). The bonds at the ends are shortest, with length 1.1583 (1.9501 Å), just as might be expected in the presence of partial double-bond character due to an unpaired electron. Subsequent bonds alternate in length going toward the center bond of the diradical: 1.2352 (2.0796 Å), 1.2192 (2.0526 Å), 1.2178 (2.0503 Å), 1.2224 (2.0580 Å), 1.2171 (2.0491 Å). The existence of this helical diradical makes it plausible that by successive additions of sulfur atoms at its ends, helical polymers of the type observed crystallographically for fibrous sulfur<sup>11</sup> would also form with the present interaction model, Eq. (2.1).

Table I summarizes the optimal cluster energies found, denoted by  $\Phi_0(n)$ . The results are also displayed on a per-atom basis,  $\Phi_0(n)/n$ . Presumably this latter quantity should pass through a minimum at  $n = 8$  to be consistent with the observed low-temperature stability of  $S_8$ . It does not, though

TABLE I. Potential energies  $\Phi_0(n)$  for globally optimal clusters of  $n$  sulfur atoms.<sup>a</sup>

$n$	$\Phi_0(n)^b$	$\Phi_0(n)/n$
2	-1.000 000 0	-0.500 000 0
3	-1.514 616 6	-0.504 872 2
4	-2.082 196 7	-0.520 549 1
5	-2.720 441 1	-0.544 088 2
6	-3.286 109 1	-0.547 684 8
7	-3.857 711 1	-0.551 101 5
8	-4.565 998 0	-0.570 749 7
9	-5.175 888 4	-0.575 098 7
10	-5.811 772 8	-0.581 177 3
12	-6.826 258 9	-0.568 854 9

<sup>a</sup>The search is thought to be complete only for  $n < 9$ .

<sup>b</sup>The energy unit is equivalent to 100.797 kcal/mol

values for  $n = 8, 9$ , and  $10$  are all quite close. We believe that small modifications in  $v_2$  and  $v_3$  can rectify this shortcoming.<sup>23</sup> In any case, the mechanically stable structures obtained closely resemble those found in real sulfur, and should indeed be reasonably close in absolute energy. For this feasibility study of bond stability and thermal disruption, the present model is useful for molecular dynamics application in its own right, as well as encouraging that improvements could be made in a subsequent version.

### III. TRANSITION STATES

Because the study of chemical reactivity is an obvious possibility with the present model, it is important to examine elementary bond cleavage processes. We have done this with sets of constrained energy minimizations for  $S_6$  and  $S_8$  clusters. Starting with the global cluster minimum reported in Sec. II, a puckered ring for both  $S_6$  and  $S_8$  cases, we fix one of the distances between a pair of bonded atoms (say  $r_{12}$  between atoms 1 and 2). For various choices of  $r_{12}$  then the cluster potential energy is minimized with respect to all other unconstrained degrees of freedom. The results can then be displayed vs  $r_{12}$  to show the effect of stretching the bond to the breaking point and beyond.

Figure 4 shows our results for bond cleavage in cyclic  $S_6$ . The absolute minimum in the curve naturally occurs at the equilibrium bond length for the unconstrained chair-form hexagon ( $r_{12} = 1.2199$ ). The constrained-minimum potential energy rises with increasing bond length  $r_{12}$  until a maximum is encountered at

$$r_{12}^{\ddagger}(S_6) = 1.697. \quad (3.1)$$

This is the transition state for the bond cleavage process. The barrier height for this transition state is 0.1612 energy units (16.24 kcal/mol).

As  $r_{12}$  in Fig. 4 continues to increase beyond its transition state value, potential energy declines until a broad relative minimum near  $r_{12} = 2.97$  is encountered. This secondary minimum corresponds to a diradical chain form of  $S_6$ . Continuing to move apart the chain ends causes a discontinuity in the optimized potential at  $r_{12} \cong 4.10$ , as the atoms suddenly shift into another chain conformation.

The maximum shown in Fig. 4 at  $r_{12} \cong 5.40$  and the sudden subsequent drop heralds breakage of a second bond.

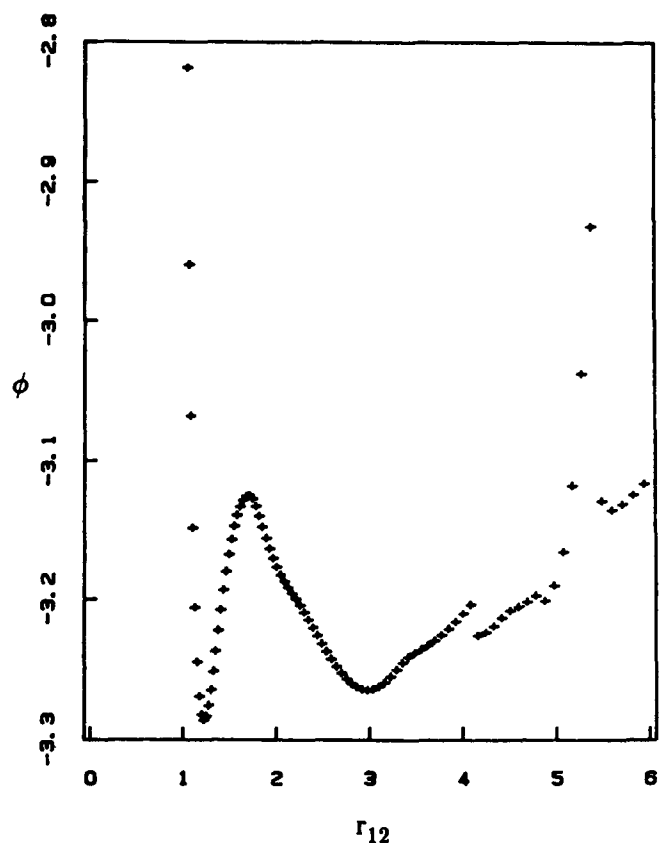


FIG. 4. Minimum energies for  $S_6$  subject to the constraint of fixed bond length  $r_{12}$ .

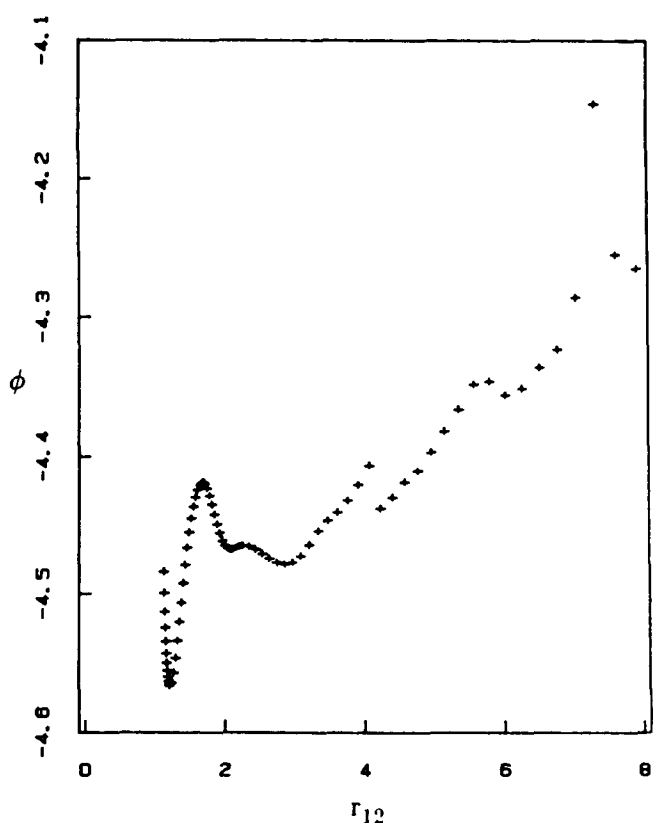


FIG. 5. Minimum energies for  $S_8$  subject to the constraint of fixed bond length  $r_{12}$ .

This is the point at which the severely stretched chain breaks apart into  $S_2$  and an  $S_4$  chain.

Figure 5 presents analogous results for bond cleavage in  $S_8$ . The minimum in the curve shown corresponds to the unconstrained cyclic sulfur octamer, all of whose bonds have length  $r_e = 1.2236$ . As might have been expected, the variation with  $r_{12}$  of the constrained-minimum potential energies is more elaborate than for the preceding case.

The transition state for cleavage of the first bond in  $S_8$  occurs at

$$r_{12}^\ddagger(S_8) = 1.688, \quad (3.2)$$

equivalent to  $2.842 \text{ \AA}$ , and entails a barrier height (relative to  $\Phi$  at  $r_e$ ):

$$\Delta\Phi^\ddagger = 0.1472, \quad (3.3)$$

equivalent to  $14.84 \text{ kcal/mol}$ . No direct gas-phase measurements or quantum mechanical calculations of this quantity are available for comparison.

As the resulting octameric chain stretches with increasing  $r_{12}$ , it manifests in sequence: (a) a relative potential minimum at approximate distance 2.09; (b) a relative maximum at approximate distance 2.26; (c) a jump discontinuity at approximate distance 4.10; (d) a relative maximum at approximate distance 5.65; (e) a relative minimum at approximate distance 6.10; (f) cleavage of the second bond, when  $r_{12} \cong 7.40$ , to create  $S_2$  and an  $S_6$  chain.

While the configurational pathway traced out by the fixed- $r_{12}$  constrained minimization passes through the exact transition state for bond scission, it should be stressed that generally this path is not the reaction coordinate. The direction of the latter through a transition state is identical (when all particles have equal masses) with the principal direction of negative curvature for the potential energy hypersurface.

In order to gain extra insight into the geometric arrangement of steepest-descent basins near the  $S_8$  ring-opening transition state, the constrained-minimum cluster configuration can serve as a set of initial configurations for unconstrained minimizations. This permits identification of the basins through which the constrained-minimization pathway sequentially passes. Figure 6 shows the results for the  $S_8$  case. Whenever  $r_{12}$  for the initial configuration is less than  $r_{12}^\ddagger(S_8)$ , Eq. (3.2), the unconstrained minimization causes the cluster to return to its fully bonded cyclic structure. For  $r_{12}$  slightly exceeding  $r_{12}^\ddagger$ , the unconstrained steepest descent converges instead to a new minimum corresponding to a folded  $S_8$  chain. Even larger  $r_{12}$  shows exiting from this second basin and penetration of a third basin, in spite of the fact that no corresponding feature is visible in the curve of constrained potentials. Evidently the potential energy surface is quite complicated even for an isolated  $S_8$  molecule.

#### IV. MOLECULAR DYNAMICS PROTOCOL

Our molecular dynamics investigations of the sulfur model all have utilized 1000 atoms in a cubical container, at whose walls periodic boundary conditions apply. The density was chosen to correspond to real liquid sulfur at  $120^\circ\text{C}$ , for which the mass density is  $1.805 \text{ g/cm}^3$ .<sup>24</sup> In our reduced units this implies a number density

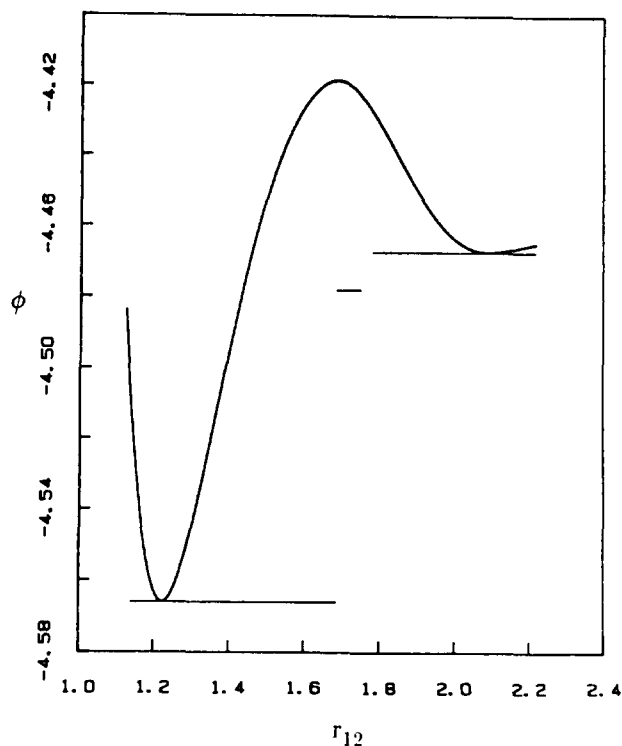


FIG. 6. Constrained minimization energies (smooth curve) for  $S_8$  ring opening, and unconstrained (basin-identifying) energies (horizontal lines) using constrained cluster configurations as initial conditions.

$$\rho = 0.16178, \quad (4.1)$$

and the corresponding cube edge is  $18.3524$  ( $30.98 \text{ \AA}$ ).

We have already introduced energy and length units ( $\epsilon$  and  $\sigma$ ) in Sec. II. The natural time unit ( $\tau$ ) is given by

$$\tau = \sigma(m/\epsilon)^{1/2}, \quad (4.2)$$

where  $m$  is the atomic mass, which we have assumed is that appropriate for the most common stable isotope  $S^{32}$ . Consequently,

$$\tau = 4.6367 \times 10^{-14} \text{ s}. \quad (4.3)$$

This time may be compared with the vibrational period that has been measured<sup>19</sup> for the sulfur dimer  $S_2$  (with the same isotope), namely  $4.5968 \times 10^{-14} \text{ s}$ .

Classical equations of motion for the 1000 sulfur atoms were integrated numerically using the fifth-order Gear algorithm.<sup>25</sup> The time increment for this integration was chosen to be

$$\Delta t = 0.005\tau. \quad (4.4)$$

For most of our molecular dynamics runs (typically  $500\Delta t$  to  $2000\Delta t$ ) this would assure constancy of the total energy to at least eight significant figures.

Following the usual procedure, changes in total energy (and hence in temperature) from one run to the next were effected by scaling all atom momenta with an appropriate common factor.

The matter of initial conditions for molecular dynamics sequences is particularly important for sulfur. This stems from the sluggishness of chemical reaction rates at low temperatures. We have utilized two distinct starting configurations in the present work. The first involves 125 intact  $S_8$

rings, and was prepared by stepwise molecular dynamics compression of a dilute assembly of  $S_8$  molecules in a cubic array, to the desired density [Eq. (4.1)]. The second placed the 1000 sulfur atoms at the vertices of a simple cubic lattice, with random momenta, to test the propensity for the atoms to self-assemble into recognizable molecules.

## V. LIQUID STRUCTURE

One of the first objectives in using molecular dynamics simulation for our sulfur model is to investigate short-range order in the liquid. The conventional measure of short-range order is the atomic pair correlation function  $g(r)$ . If the liquid was prepared initially from intact cyclic  $S_8$  molecules, and the temperature remained low, these molecules should continue to be present as such on any reasonable simulation time scale.

In our reduced units, the thermodynamic melting temperature (115.1 °C) is equal to

$$T_m^* = k_B T_m / \epsilon = 7.6576 \times 10^{-3}. \quad (5.1)$$

Experimentally the liquid can readily be supercooled.<sup>26</sup> Figure 7 shows  $g(r)$  computed for a moderately supercooled melt at reduced temperature  $7.144 \times 10^{-3}$  (89.1 °C), which in fact consists entirely of intact cyclic  $S_8$  molecules. Its most prominent feature is a narrow isolated peak centered near reduced distance 1.22. This represents all covalent pair bonds present in the system, and numerical integration shows that just the expected number of such bonds, 1000, exists. The other features shown in Fig. 7 are distinctive but less prominent peaks, the next two of which (reduced distances around 2.0 and 2.9) would be expected to include nonbonded intramolecular pairs within the same  $S_8$  ring.

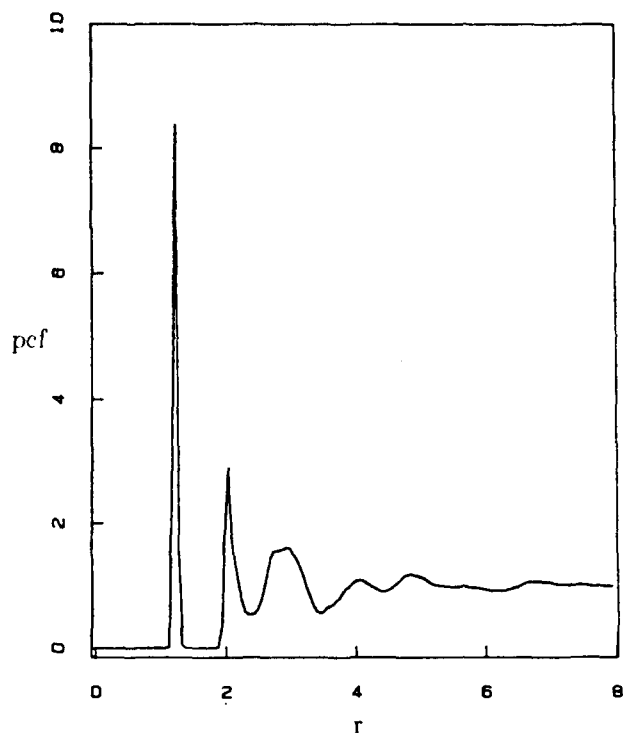


FIG. 7. Pair correlation function for (slightly supercooled) liquid sulfur at reduced temperature  $7.144 \times 10^{-3}$  (89.1 °C). The melt consists entirely of cyclic  $S_8$  molecules.

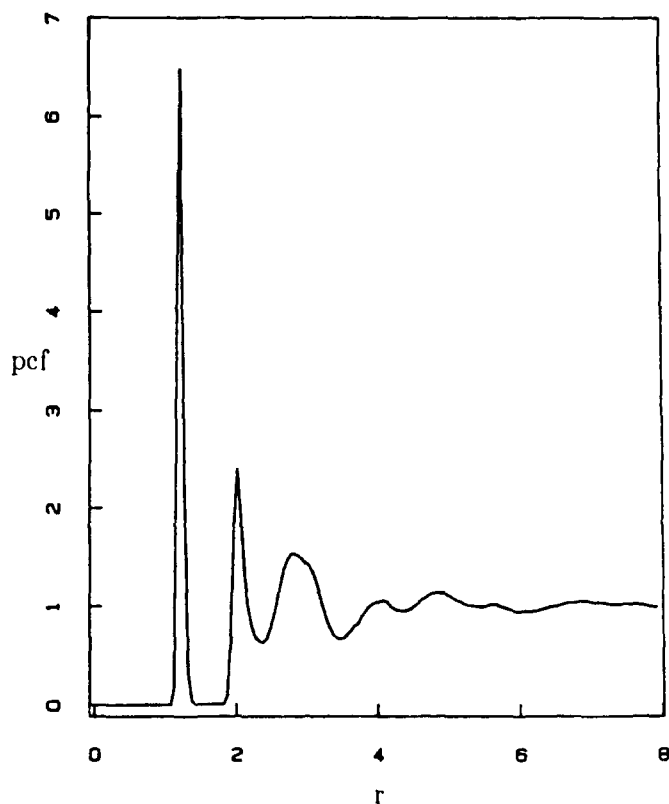


FIG. 8. Pair correlation function for liquid sulfur heated quickly to reduced temperature  $1.5250 \times 10^{-2}$  (500.1 °C). No reaction has occurred yet; the liquid still consists entirely of cyclic  $S_8$  molecules.

However, intermolecular pairs should also be expected to occur in this range, between neighboring  $S_8$  rings.

Raising the temperature naturally causes the short-range order in  $g(r)$ , both intramolecular and intermolecular, to become less distinctive. However as long as the molecular composition remains entirely cyclic  $S_8$ , the changes are relatively modest. Figure 8 shows  $g(r)$  for a hot liquid of this composition that was heated rapidly to reduced temperature  $1.5250 \times 10^{-2}$  (500.1 °C). Although peak amplitudes have diminished, the resemblance to the preceding Fig. 7 for the cold liquid is indeed close. Most important perhaps is that the gap has narrowed between the peak for covalent intramolecular bonded pairs, and the nonbonded remainder of the pair distribution. It is clear that the change for a bonded pair to traverse this gap (i.e., for the bond to cleave) has substantially increased.

If the temperature were to remain at this last value, or to rise, the cyclic  $S_8$  molecules would begin to react chemically during the time available in molecular dynamics simulation. The sulfur system was in fact heated from the state illustrated in Fig. 8 at roughly a uniform rate (in stages) to reduced temperature  $3.0406 \times 10^{-2}$  (1269 °C), during which heating  $3.2 \times 10^4$  integration steps  $\Delta t$  elapsed (7.44 ps). Subsequently, the system was allowed to evolve at constant energy for  $2 \times 10^4 \Delta t$  (4.64 ps). Figure 9 shows  $g(r)$  averaged over the last  $2 \times 10^3 \Delta t$  of this final sequence, during which the mean reduced temperature was  $3.0246 \times 10^{-2}$  (1261 °C).

The pair correlation functions for the lower temperatures shown in Figs. 7 and 8 numerically equal zero in the gap between the first peak for covalently bonded pairs, and

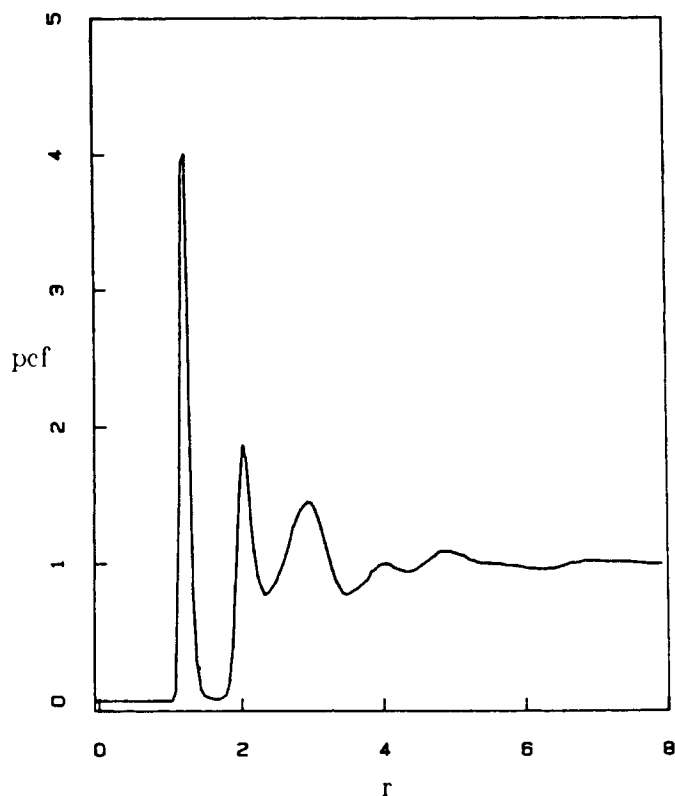


FIG. 9. Pair correlation function for the hot reacting fluid at reduced temperature  $3.0246 \times 10^{-2}$  (1261 °C).

the subsequent second peak for nonbonded pairs. That is no longer the case for the hot-system  $g(r)$  shown in Fig. 9, where the minimum  $g$  value achieved in this range is approximately  $1 \times 10^{-2}$ . Obviously sulfur pairs have begun to invade and to move across the "forbidden zone" at a perceptible rate. Chemical reaction is underway.

Reduced distance 1.50 (2.5452 Å) offers a convenient cutoff criterion for the purpose of enumerating covalent bonds. This distance lies near the center of the low-temperature forbidden zone. Consequently it seems reasonable to count all pairs of atoms  $i, j$  as bonded, if and only if

$$r_{ij} < 1.50. \quad (5.2)$$

As implied above, this criterion leads to identification of exactly the expected 1000 bonds for the intact  $S_8$  rings in the states shown in Figs. 7 and 8. That is not the case, though, for the state shown in Fig. 9. Applying criterion (5.2) to the atomic configuration at the end of that molecular dynamics run, we find that only 947 bonds are present.

With a criterion for bonding in hand, it is possible to partition the 1000 sulfur atoms into molecular subsets, i.e., groupings mutually connected by chemical bonds. When this is done for the atomic configurations appearing during the low temperature molecular dynamics runs, all 125  $S_8$  rings are identified as such. The final configuration from the reacting high-temperature state, Fig. 9, presents quite a different picture, however. Only 31 cyclic  $S_8$  molecules have survived, while many chains of different lengths have been created. These latter include 14 octameric chains, presumably formed directly by bond cleavage from rings. But in addi-

tion we find chains of 2 to 45 sulfur atoms, with the existence of the larger sizes demonstrating that the model has the capacity at least qualitatively to exhibit spontaneous polymerization at high temperature. Finally, the reacting medium is also found to contain a tadpole structure (with a formally trivalent sulfur), whose role we discuss in Sec. VI.

Since  $g(r)$  can be quite accurately determined for our sulfur model by the molecular dynamics simulation, it would be helpful if meaningful comparisons could be made with experimental determinations of this function. While some experimental results have in fact been published<sup>27,28</sup> they are far too imprecise to be useful. All that we can conclude is that rough qualitative agreement seems to obtain. A strong need now exists for state-of-the-art diffraction experiments, with careful data reduction, to show accurately how  $g(r)$  looks for real liquid sulfur at various temperatures.

## VI. QUENCHED STATES

At very high temperature, where  $g(r)$  is positive at the cut-off distance 1.5, there may be some concern about whether this cutoff has been placed in exactly the proper position to enumerate bonds "correctly." In this circumstance the number of bonds present will not be invariant to a small displacement in that cutoff, leading to some ambiguity. However we can remove this ambiguity by subjecting any atomic configuration to the mapping that forms the basis of the "inherent structure" formalism for liquids.<sup>14-18</sup> This mapping in principle utilizes a steepest-descent relaxation of a starting configuration, to reduce it to the mechanically stable configuration of a potential energy minimum. This process removes thermally induced vibrational distortion, and at least for simple atomic liquids it has the effect of substantially sharpening the image of short-range order conveyed by the pair correlation function.<sup>16</sup>

We now verify that the same sharpening applies to the liquid sulfur model as well. Starting from the final configuration of the  $T = 7.1441 \times 10^{-3}$  supercooled liquid represented by Fig. 7, the equations of atomic motion were numerically damped so that the system would settle quickly into a nearby potential energy minimum. The pair correlation function for the resulting single system configuration was then evaluated. It is presented in Fig. 10. The potential energy of this solid amorphous packing is

$$\Phi = -656.51647. \quad (6.1)$$

In comparison with its prequench predecessor, Fig. 7, short-range order has indeed sharpened, as the rise in the first peak from 8.4 to 13.0 indicates. More significant is the resolution of the second peak into two overlapping components, the inner one of which we identify as intramolecular second neighbors, and the outer one of which we identify as intermolecular contact van der Waals pairs. Needless to say, bonding criterion (5.2) continues to show after quenching that 1000 covalent bonds are present, organizing the sulfur atoms into exactly 125 cyclic  $S_8$  molecules.

Final-configuration quenches from other unreacted liquid states have also been examined, and they consistently show pair correlation functions closely resembling that in

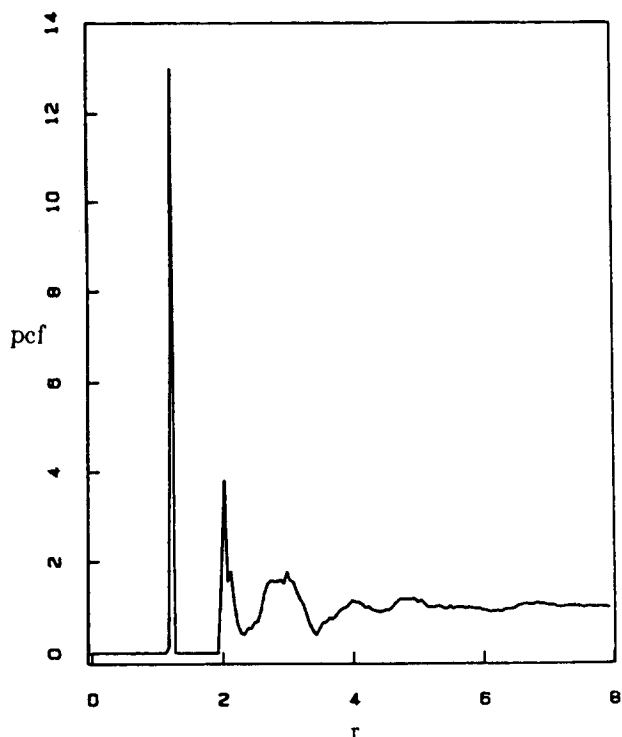


FIG. 10. Pair correlation function for the mechanically stable structure obtained by quenching the supercooled liquid at reduced temperature  $7.1441 \times 10^{-3}$  (89.1 °C).

Fig. 10. In particular, the partial resolution of the second peak is a robust feature. Provided one stays within the unreacted manifold of liquid states, sulfur appears to mimic the behavior of simpler liquid models: temperature dependence of the thermodynamic-state pair correlation functions re-

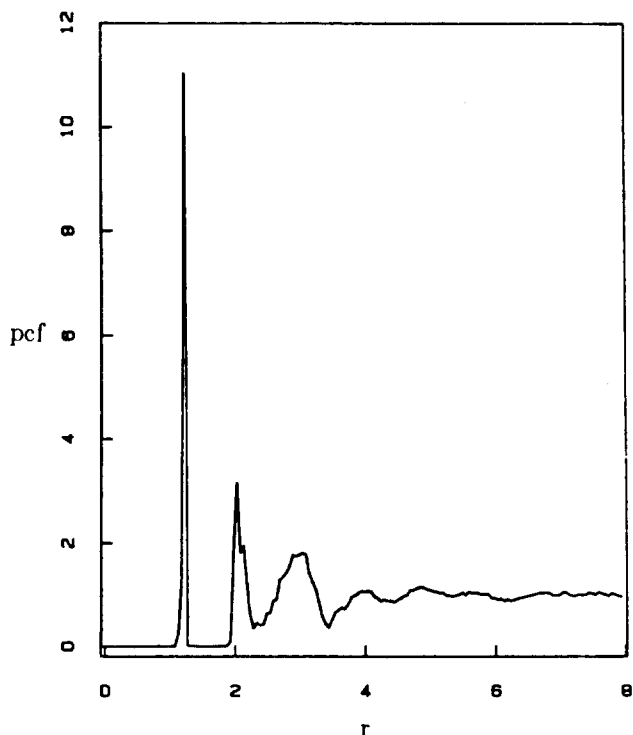


FIG. 11. Pair correlation function for the potential energy minimum obtained by quenching the partially reacted fluid at reduced temperature  $3.0246 \times 10^{-2}$  (1261 °C).

sides primarily in the varying extents of vibrational deformation, and is substantially removed by steepest-descent quenching.<sup>14-18</sup> That is, the unreacted liquid seems to possess a temperature-independent inherent structure.

Figure 11 shows the pair correlation function for the quenched configuration obtained from the end of the reaction sequence at reduced temperature  $3.0246 \times 10^{-2}$  (1261 °C). The value of the potential energy at this relative minimum is substantially higher than that given by Eq. (6.1) above:

$$\Phi = -649.63743. \quad (6.2)$$

The covalent-bond peak has again risen in comparison with its precursor in Fig. 9, but only to 11.0. Once again the second peak is partially resolved into a pair of overlapping components. The third peaks in both Figs. 10 and 11 are broad but appear to have significantly different shapes, the latter case being narrower.

The most important conclusion that emerges from comparison of Figs. 9 and 11 is that quenching to potential minima clears pairs out the forbidden zone. The quench pair correlation function in Fig. 11 numerically vanishes over the range

$$1.375 < r < 1.875, \quad (6.3)$$

which comfortably spans the cut-off distance 1.50. Consequently the quenching has removed bonding ambiguity. For the case in hand, the quench possesses 951 bonds, all substantially shorter than the cutoff. Since only 947 bonds satisfied the criterion before the vibrational deformation in the system was removed, it is clear that a few bonds have relaxed across the cutoff.

Table II shows for the reacted fluid the molecular species identified by criterion (5.2) that are present both before and after the quench. The 12-atom "other structure" that appears both before and after removal of vibrational deformation has been identified as a tadpole formed by weak attachment of one end of an  $S_4$  diradical chain to one atom of an  $S_8$  ring. We have observed tadpole species in other prequench and postquench configurations as well. Figure 12 shows a picture of such a tadpole extracted from another quench (with lesser extent of reaction), clearly showing the formally trivalent sulfur.

TABLE II. Molecular species in the partially reacted fluid at reduced temperature  $3.0246 \times 10^{-2}$  (1261 °C).

Open chains	
Prequench:	$4S_2, 2S_3, S_4, S_5, 3S_6, 14S_8, S_9, S_{10}, S_{11}, 2S_{12}, 3S_{14}, S_{15}, 2S_{16}, 2S_{18}, S_{19}, S_{20}, 2S_{21}, S_{22}, S_{23}, S_{24}, 2S_{27}, S_{28}, 2S_{32}, S_{33}, S_{34}, S_{45}$
Postquench:	$3S_2, 2S_3, S_4, S_5, 3S_6, 12S_8, S_9, S_{10}, S_{11}, 2S_{12}, 3S_{14}, 2S_{16}, 2S_{18}, S_{19}, S_{20}, 2S_{21}, S_{22}, S_{24}, S_{27}, S_{28}, S_{29}, 2S_{32}, S_{33}, S_{34}, S_{38}, S_{45}$
Simple cycles	
Prequench:	$31S_8$
Postquench:	$33S_8$
Other structures	
Prequench	$S_{12}$
Postquench:	$S_{12}$



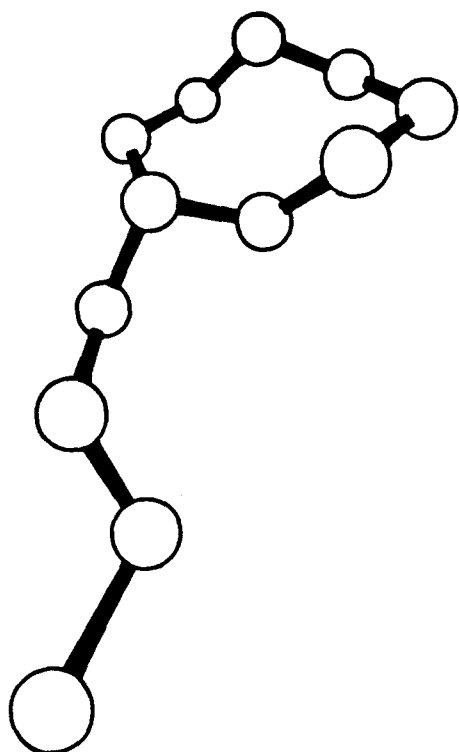


FIG. 12. Tadpole structure for  $S_{12}$  extracted from a quenched configuration at the beginning of a reaction sequence.

The 12-atom configuration shown in Fig. 12 was utilized as the starting point for a potential-energy minimizing routine for this small atom grouping alone. The objective was to see if such an object could be mechanically stable by itself, or if it required the interactions with the neighboring medium to hold it together. In fact we found that there is a tadpole relative minimum for 12 sulfur atoms with our model interaction, with a conformation differing only little from that shown in Fig. 12. Its potential energy is found to be

$$\Phi(\text{tadpole}) = -6.588\,782\,9. \quad (6.4)$$

Comparison with results in Table I shows that this is substantially higher than the potential energy of cyclic  $S_{12}$  in its optimal conformation. We also find that result (6.4) lies higher than the sum of optimized cluster energies for the two parts of the tadpole, namely cyclic  $S_8$  and the most favorable  $S_4$  chain; the increment is found to be

$$\Delta\Phi = 0.059\,411\,8, \quad (6.5)$$

or about 6 kcal/mol in conventional units. Thus, the tadpole has local mechanical stability, but it is metastable with respect to breakup into the two component parts.

Nevertheless the tadpole structures with temporarily trivalent sulfur may be important reaction intermediates in degradation of cyclic  $S_8$ . The optimized  $S_{12}$  tadpole structure exhibits three anomalously long and weak bonds at the trivalent sulfur vertex. If thermal processes have created such a tadpole in the medium, roughly speaking there will be two chances out of three that subsequently a weakened bond in the ring portion of the tadpole will cleave to yield an open chain. We believe this mechanism is important for the polymerization kinetics in our model, and possibly in real sulfur as well.

## VII. DISCUSSION

The present project should be viewed as a feasibility study, intended to establish that standard computer simulation methods could be applied to study chemical structure and reactivity in condensed phases of sulfur. Results obtained are encouraging in that relatively simple two- and three-body atomic interactions suffice (at least qualitatively) to represent the elaborate molecular structures for this element, and they offer an efficient format for use in molecular dynamics applications. The model interactions are imperfect, but they can undoubtedly be improved. In particular our most recent work along these directions shows that small modifications are possible which render cyclic  $S_8$  more stable (on a per-atom basis) than any other isolated cluster of 12 or fewer atoms. This change is necessary to accord with the absolute stability experimentally observed for this species in the low-temperature crystalline phase. In the future, we expect to try to tailor the two- and three-body interactions to reproduce known crystal structures, cohesive energies, and elastic constants.

In view of structural similarities between S and Se in their solid phases,<sup>11</sup> no doubt there is a similar way to represent atomic interactions in the latter substance. Scientifically this could have important consequences for better understanding of amorphous Se.

Even in its present imperfect version, the sulfur model obviously has the capacity to produce linear polymers. This capacity was already clear in the cluster studies reported in Sec. II, and was illustrated again by the thermally induced formation of polymers during the molecular dynamics, as revealed for example in Table II. We have also observed spontaneous polymerization to occur when the sulfur molecular dynamics is initiated from a very different and unnatural configuration, namely a simple cubic lattice. The point is that this type of model may be particularly helpful for simulating polymer coiling statistics and relaxation dynamics. By simple extension, it would be possible to include inert solvent molecules in the model, and to implement molecular dynamics of a long linear polymer in that solvent. At low temperature such a linear polymer would undergo Brownian motion, but should not suffer bond breakage.

Although we have been able to observe chemical reactions proceeding at elevated temperatures (600 °C and above), primary interest for sulfur really lies in the temperature range between the melting point and neighborhood of the fascinating lambda transition (i.e., below 200 °C). Reaction rates in pure sulfur both in the laboratory and for our model are so much slower in this latter temperature range that on the typical molecular dynamics time scale they would be totally unobservable. Consequently there is no hope by conventional computer simulation means of monitoring the shifting chemical equilibria that determine the lambda transition at 159 °C.

However this otherwise pessimistic situation presents an exciting optimistic prospect, namely that a mathematical catalyst could be introduced in the simulations to speed up rates to a more acceptable regime. One way of implementing this idea might be to insert a "mutant sulfur atom," with interactions modified to lower reaction barriers and to en-

courage trivalency. If this strategy were successful, the resulting study of low-temperature sulfur equilibria by molecular dynamics could be a valuable supplement to existing theories of the lambda transition.<sup>29,30</sup>

<sup>1</sup>S. W. Benson, *Foundations of Chemical Kinetics* (McGraw-Hill, New York, 1960).

<sup>2</sup>V. N. Kondrat'ev, *Chemical Kinetics of Gas Reactions*, translated from the Russian by J. M. Crabtree and S. N. Carruthers (Pergamon, Oxford, 1964).

<sup>3</sup>J. P. Hansen and I. R. McDonald, *Theory of Simple Liquids* (Academic, New York, 1976), Chap. 3.

<sup>4</sup>F. H. Stillinger and A. Rahman, *J. Chem. Phys.* **60**, 1545 (1974).

<sup>5</sup>T. A. Weber and E. Helfand, *J. Chem. Phys.* **71**, 4760 (1979).

<sup>6</sup>J. Chandrasekhar and W. L. Jorgensen, *J. Chem. Phys.* **77**, 5073 (1982).

<sup>7</sup>S. F. Trevino and D. H. Tsai, *J. Chem. Phys.* **81**, 248 (1984).

<sup>8</sup>D. L. Bunker and B. S. Jacobson, *J. Am. Chem. Soc.* **94**, 1843 (1972); see also A. J. Stace and J. N. Murrell, *Mol. Phys.* **33**, 1 (1977).

<sup>9</sup>J. Chandrasekhar, S. F. Smith, and W. L. Jorgensen, *J. Am. Chem. Soc.* **106**, 3049 (1984).

<sup>10</sup>R. Steudel, *Studies in Inorganic Chemistry 5*, edited by A. Müller and B. Krebs (Elsevier, New York, 1974), pp. 3-37.

<sup>11</sup>J. Donohue, *The Structures of the Elements* (Krieger, Malabar, FL, 1982), Chap. 9.

<sup>12</sup>R. Steudel, *Top. Curr. Chem.* **102**, 149 (1982); see especially Sec. 7.

<sup>13</sup>J. A. Poulis and C. H. Massen, in *Elemental Sulfur, Chemistry and Physics*, edited by B. Meyer (Wiley-Interscience, New York, 1965), Chap. 6.

<sup>14</sup>F. H. Stillinger and T. A. Weber, *Phys. Rev. A* **25**, 978 (1982).

<sup>15</sup>F. H. Stillinger and T. A. Weber, *Phys. Rev. A* **28**, 2408 (1983).

<sup>16</sup>F. H. Stillinger and T. A. Weber, *J. Chem. Phys.* **80**, 4434 (1984).

<sup>17</sup>F. H. Stillinger and T. A. Weber, *Science* **225**, 983 (1984).

<sup>18</sup>F. H. Stillinger and T. A. Weber, *Phys. Rev. B* **31**, 5262 (1985).

<sup>19</sup>K. P. Huber and G. Herzberg, *Molecular Spectra and Molecular Structure. IV. Constants of Diatomic Molecules* (Van Nostrand Reinhold, New York, 1979), p. 564.

<sup>20</sup>We have used the nonproprietary "MINOP" procedure (L. Kaufmann, AT&T Bell Laboratories, 1980), which optimally alternates between steepest-descent and quasi-Newton methods.

<sup>21</sup>Z. S. Herman and K. Weiss, *Inorg. Chem.* **14**, 1592 (1975).

<sup>22</sup>R. Steudel, J. Steidel, J. Pickardt, F. Schuster, and R. Reinhardt, *Z. Naturforsch. Teil B* **35**, 1378 (1980).

<sup>23</sup>Our recent studies show this presumption is correct.

<sup>24</sup>A. M. Kellas, *J. Chem. Soc.* **113**, 903 (1918).

<sup>25</sup>C. W. Gear, *Numerical Initial-Value Problems in Ordinary Differential Equations* (Prentice-Hall, Englewood Cliffs, 1971).

<sup>26</sup>*The Sulphur Data Book*, edited by William N. Tuller (McGraw-Hill, New York, 1954), p. 12.

<sup>27</sup>C. W. Tompson and N. S. Gingrich, *J. Chem. Phys.* **31**, 1598 (1959).

<sup>28</sup>Yu. G. Poltavtsev and Yu. V. Titenko, *Russ. J. Phys. Chem.* **49**, 178 (1975).

<sup>29</sup>A. V. Tobolsky and A. Eisenberg, *J. Am. Chem. Soc.* **81**, 780 (1959).

<sup>30</sup>J. C. Wheeler and P. Pfeuty, *Phys. Rev. A* **24**, 1050 (1981).